Journal of Organometallic Chemistry 693 (2008) 3509–3518

Contents lists available at ScienceDirect

Journal of Organometallic Chemistry

journal homepage: www.elsevier.com/locate/jorganchem

Zirconium complexes with versatile β-diketiminate ligands: Synthesis, structure, and ethylene polymerization

Shaogang Gong, Haiyan Ma *, Jiling Huang *

Laboratory of Organometallic Chemistry, East China University of Science and Technology, 130 Meilong Road, Shanghai 200237, People's Republic of China

ARTICLE INFO

Article history:
Received 28 May 2008
Received in revised form 4 August 2008
Accepted 18 August 2008
Available online 26 August 2008

Keywords:
β-Diketiminate
Zirconium
Polyethylene
Catalysis
Polymerization

ABSTRACT

A series of zirconium complexes (**2c**, **2d**, **2f**, **2g**, **2h**, **2i**) containing symmetrical or unsymmetrical β-diketiminate ligands were synthesized by the reaction of $ZrCl_4 \cdot 2THF$ with lithium salt of the corresponding ligand in 1:2 molar ratio. X-ray crystal structures reveal that complexes **2d** and **2g** adopt distorted octahedral geometry around the zirconium center. These complexes showed moderate activities for ethylene polymerization, when methylaluminoxane (MAO) was used as cocatalyst. The steric and electronic effects of the substituents at the phenyl rings had considerable influence on the catalytic activities of the metal complex, as well as the molecular weights and molecular weight distributions (MWD) of produced polymers. Introduction of electron-withdrawing CF_3 group to phenyls in the ligand led to a significant increase of catalytic activities, and complex **2f** (*p*-CF_3) exhibited the highest catalytic activity of 7.45×10^5 g PE/mol-Zr · h among the investigated complexes. Complexes **2a**–**d** could produce ultra-high molecular weight polyethylenes (UHMWPE) that were hardly dissolvable in decahydronaphthalene or 1,2-dichlorobenzene under the molecular weight measurement conditions. Nevertheless, polyethylenes with broad MWD could be afforded by complexes **2g**–**i**, which was probably due to the introduction of bulky unsymmetrical ligands leading to the formation of multi active species under polymerization conditions. High-temperature ^{13}C NMR data indicate the linear structure of obtained polyethylenes.

© 2008 Elsevier B.V. All rights reserved.

1. Introduction

Over the past decades, considerable development of olefin polymerization catalysts of high-performance has created a variety of polymers with novel properties. For example, ultra-high molecular weight polyethylenes (UHMWPE) having a molecular weight (M_w) greater than 3 000 000 possess excellent abrasion resistance and impact strength, very low coefficient friction, good self-lubricants properties, as well as good resistance at low temperature [1–8]. Polyethylenes with broad or multi-model molecular weight distribution (MWD) can meet the requirement for good resin processability, since they show high workability due to the high molecular weight (HMW) fractions, and at the same time they provide excellent mechanical properties due to the low molecular weight (LMW) fractions [9,10]. Therefore, many academic and industrial research laboratories have engaged in the design and synthesis of organometallic pre-catalysts of special structure with the aim to obtain polyolefins possessing high-performance [11].

Recently, interests grow in developing new generation "non-metallocene" catalysts, partly to avoid the growing patent minefield in group 4 cyclopentadienyl (Cp) systems, but most importantly to explore the potential of metal complexes with other ligands except for Cp to polymerize ethylene and other olefinic monomers [11]. Thereinto, β-diketiminate ligands attract considerable attention due to their isoelectronic relationship with cyclopentadienyl anion, easily preparing from cheap and readily available materials, as well as easy modulation of steric and electronic requirements by varying the amine moieties and the backbone [12–25]. Up to the present, a number of group 4 complexes bearing β-diketiminate ligands have been synthesized and used as pre-catalyst for olefin polymerization [17]. For example, in 1996 Lappert's group [26] synthesized *N*-trimethylsilyl substituted β-diketiminate zirconium and hafnium complexes, which showed high activities in ethylene polymerization and moderate activities in 1-hexene homopolymerization and copolymerization with ethylene [27]. Then Collins [28] and Andres's [29] groups synthesized mono-, bis(β-diketiminate) complexes and monocyclopentadienyl β-diketiminate mixed complexes of group 4 metals. It was found that monocyclopentadienyl β-diketiminate zirconium complexes with electron-withdrawing group in *N*-aryl moiety showed the highest catalytic activity for ethylene polymerization [30]. What's more, Smith's [31] and Mindiola's [32] groups reported the synthesis of some five- and six-coordinate group 4 β-diketiminate complexes, where molecular structures in the solid state and in solution, and intermolecular rearrangement reactions were further investigated [33]. Besides, Berke et al. [34] found that volatile

* Corresponding authors. Tel./fax: +86 21 64253519.
E-mail addresses: haiyanma@ecust.edu.cn (H. Ma), qianling@online.sh.cn (J. Huang).

0022-328X/$ - see front matter © 2008 Elsevier B.V. All rights reserved.
doi:10.1016/j.jorganchem.2008.08.024

β-diketiminate bis(dialkylamido)zirconium complexes could be utilized as potential precursors in metal-organic chemical vapor deposition processes (MOCVD). Novak [35], Liu [36] and Xie's [37] groups prepared zirconium, titanium trichloride complexes with mono β-diketiminate ligand possessing different aromatic or aliphatic substituents, and found that complexes of aliphatics-substituted β-diketiminate ligand displayed higher catalytic activity; fluoro-substituted titanium complex displayed higher activities for ethylene/1-hexene copolymerization than for ethylene homopolymerization [37]. In order to further explore the olefin polymerization behavior of β-diketiminate group 4 complexes, a series of analogous Ti(III) complexes were synthesized by Budzelaar's [38] and Theopold's [39] groups, which produced polyethylene with broad MWD (MWD = 28.6). Roesky's [40] and Mindiola's [41] groups investigated the stability of β-diketiminate Ti(III) complexes as well as their intermolecular rearrangement reactions. More recently, Wu's [42] and Li's [43] groups prepared the bulky bis(β-diketiminate)titanium complexes with trifluoromethyl-substituted backbone, which displayed moderate activities for the homo- and copolymerization of ethylene and norbornene.

As we know, all the previously reported β-diketiminate group 4 complexes possessed symmetrical ligand framework. Enlightened by Fujita's FI catalysts [44] with bulky *ortho*-substitutent at phenoxy moiety capable of producing polyethylenes with uni-, bi-, and trimodal MWD, we introduce bulky β-diketimines bearing two different *N*-aryl groups to zirconium metal and conceive that potential multiple metal species resulting from the versatile coordination modes of the unsymmetrical ligand could lead to the produce of polyethylenes with broad or multi-model molecular weight distribution. Here we report the synthesis of a series of novel zirconium complexes possessing symmetrical or unsymmetrical β-diketiminate ligands; the ethylene polymerization behavior of these complexes is also studied. To the best of our knowledge, it's the first time that the unsymmetrical β-diketiminate ligands are introduced to zirconium complexes.

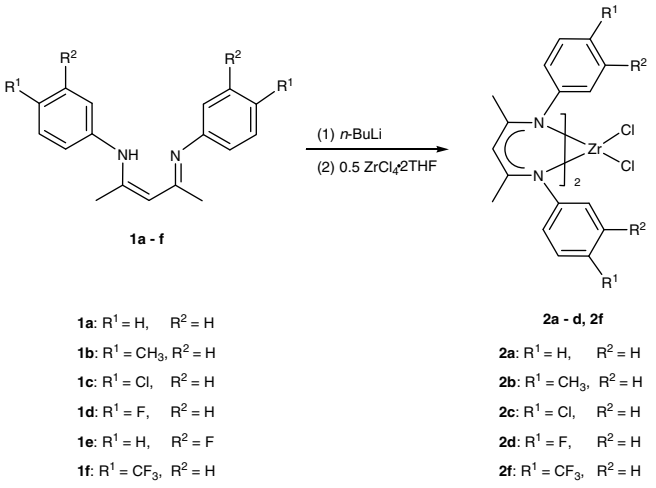

1a: R^1 = H, R^2 = H
1b: R^1 = CH_3, R^2 = H
1c: R^1 = Cl, R^2 = H
1d: R^1 = F, R^2 = H
1e: R^1 = H, R^2 = F
1f: R^1 = CF_3, R^2 = H

2a: R^1 = H, R^2 = H
2b: R^1 = CH_3, R^2 = H
2c: R^1 = Cl, R^2 = H
2d: R^1 = F, R^2 = H
2f: R^1 = CF_3, R^2 = H

Scheme 1. The synthetic route of complexes **2a–d** and **f**.

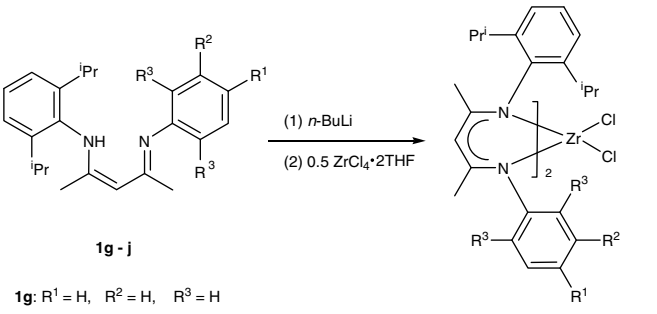

1g: R^1 = H, R^2 = H, R^3 = H
1h: R^1 = ^{i}Pr, R^2 = H, R^3 = H
1i: R^1 = H, R^2 = F, R^3 = H
1j: R^1 = H, R^2 = CF_3, R^3 = H
1k: R^1 = H, R^2 = H, R^3 = CH_3

2g: R^1 = H, R^2 = H, R^3 = H
2h: R^1 = ^{i}Pr, R^2 = H, R^3 = H
2i: R^1 = H, R^2 = F, R^3 = H

Scheme 2. The synthetic route of complexes **2g–i**.

2. Results and discussion

2.1. Synthesis of β-diketiminate ligands and β-diketiminate zirconium complexes

In order to investigate in detail the steric and electronic effect of β-diketiminate ligand on the catalytic behaviors of the corresponding complex, a series of ligands **1a–k** [18,19,45] containing different *ortho*-, *meta*-, and *para*-substituted *N*-aryl groups were utilized to synthesize the zirconium complexes. Complexes **2a** [28] and **2b** [31] were prepared according to the reported procedures in the literature. As depicted in Schemes 1 and 2, zirconium complexes **2c–d** and **g–i** bearing symmetrical or unsymmetrical auxiliary ligands were prepared in moderate yields via the reaction of $ZrCl_4 \cdot 2THF$ and two equivalents of lithium salt of the corresponding ligand in toluene [31]. These complexes with satisfactory elemental analysis were obtained as yellow to orange yellow crystalline solids after recrystallization from hot toluene. The same procedure was adopted to prepare complex **2f**, and a brown yellow solid was isolated. The ^{1}H NMR spectrum however showed an unknown compound instead of the target complex. When diethyl ether instead of toluene was used as reaction solvent, target complex **2f** was isolated successfully as orange yellow crystals and well-characterized by ^{1}H NMR and elemental analysis. In order to explore the reason, the lithium salt of **1f** prepared in toluene was hydrolyzed. To our surprise, only the *para*-trifluoromethyl aniline and some unknown compounds were detected in the hydrolyzed mixture. On the contrary, hydrolysis of the lithium salt of **1f** prepared in diethyl ether afforded ligand **1f** in high yield. Philip and coworkers ever reported [46] that the unsolvate [{(2,6-$Pr^i_2H_3C_6$)N(CH_3)C}$_2$CH]Li obtained from toluene existed as dimer or dodecamer; besides two *N*-coordination from one β-diketiminate, each Li^+ ion was associated by coordinating to one *N*-aryl carbon in another β-diketiminate ligand as evidenced by the X-ray diffraction measurement. On the other hand, the etherate [{(2,6-$Pr^i_2H_3C_6$)N(CH_3)C}$_2$CH]Li(Et_2O) crystallized as monomers featuring the Li^+ ion in a distorted trigonal planar geometry [46]. It is conceivable for us that the introduction of strong electron-withdrawing group CF_3 to the *para*-position of the phenyl ring weakened such association interaction in toluene and resulted in the decomposition of the lithium salt of **1f**. Due to the coordination effect of solvent, the etherate [{(4-$CF_3H_4C_6$)N(CH_3)C}$_2$CH]Li(Et_2O) could exist stably in diethyl ether, therefore the desired complex **2f** was afforded.

Analytically pure samples of zirconium complexes containing *meta*-fluoro substituted β-diketimine **1e** and *meta*-trifluoromethyl substituted **1j** could not be isolated using the similar procedure as that of **2a** due to the poor solubility in hot toluene or thermal instability. With the consideration that variation of the steric bulkiness of ligand may lead to profound changes in the performance of catalyst and the microstructure of produced polymers, we attempted to synthesize zirconium complex bearing **1k**. However, no reaction could be observed between the lithium salt of **1k** and $ZrCl_4 \cdot 2THF$ or $ZrCl_4$, most probably attributed to the steric hindrance [31].

Although similar β-diketiminate titanium complexes were prepared using CH_2Cl_2 as extracting solvent [37,42,43], these

zirconium complexes are quite unstable in polar solvents such as CH_2Cl_2, CH_3CN, and pyridine. In view of the poor solubility of them in toluene or benzene at room temperature, $CDCl_3$ was utilized in the ^1H NMR measurement despite of the fractional decomposition of the complexes. ^1H NMR data of complexes **2a–d**, **f** at room temperature indicate equivalent methine (γ-H) environments in both ligands, which resonate at ca. 5.4 ppm as a single peak. For complexes **2g–i** containing unsymmetrical auxiliary ligand, only one set of signals for both ligands was shown in the ^1H NMR spectra; wherein two single peaks were observed for the backbone methyls and one sharp resonance for the methine proton (γ-H) at ca. 5.8 ppm, indicating the absence of other isomers at least in solution on the NMR time scale at room temperature. In comparison with those of complexes **2a–d** and **f**, the chemical shifts of methine protons (γ-H) in complexes **2g–i** move to lower field, which probably results from the partial η^n character of the chelating N–C–C–C–N ring indicated by the significant deviation of zirconium atom from the ligand backbone plane (*vide post*).

2.2. Crystal structure of zirconium complexes **2d** and **2g**

Single crystals of zirconium complexes **2d** and **2g** suitable for X-ray diffraction measurement were obtained by slowly cooling a saturated toluene solution to 0 °C. The selected bond lengths and angles are summarized in Table 1. The molecular structures of **2d** and **2g** are shown in Figs. 1 and 2, respectively. In the solid state, complex **2d** adopts distorted octahedral geometry around the zirconium center with two *cis*-chlorine atoms at an angle of 91.08(4)°, in which the N–Zr–N angles involving single diketiminate ligand deviate significantly from 90° (N(1)–Zr–N(2) = 79.92(10)°, N(3)–Zr–N(4) = 80.25(11)°). The shorter Zr–N(3) bond distance of 2.187(3) Å in comparison with Zr–N(4) = 2.259(3) Å shows the *trans* influence of the chlorine atom [28,31]. However, the almost same bond distances of Zr–N(1) (2.238(3) Å) and Zr–N(2) (2.236(3) Å) indicate the absence of the expected *trans* influence of the chlorine. More obvious difference of two backbone C–C bond distances (C(1)–C(2) = 1.382(5), C(2)–C(3) = 1.399(5) Å) and of two N–C bond distances (N(1)–C(1) = 1.349(4), N(2)–C(3) = 1.327(4) Å) in comparison with those of **2a** [28] and **2b** [31] indicates an inferior delocalization effect, probably due to the introduction of the *para*-fluorine atoms similar as the reported fluoro-substituted mono(diiminato)titanium trichloride complex [37]. The ligand backbone in **2d** is non-planar with C(2) deviating from the least-squares plane (defined by N(1), N(2), C(1), and C(3)) by 0.1577 Å. The zirconium atom deviates from this plane by 0.7180 Å.

Similarly, in the solid state, complex **2g** also shows a distorted-octahedral geometry at the metal center with two *cis*-chlorine atoms at an angle of 89.26(5)°, which is comparable to those in **2a** [28], **2b** [31], and **2d** (90.0(1)°, 90.13(3)°, and 91.08(4)°, respectively) and slightly larger than that of the titanium congener (87.88(19)°) [43]. The average Zr–Cl bond distance of 2.4069 Å is slightly shorter than those observed in **2a**, **2b** and **2d** (2.4325, 2.4371 and 2.4221 Å, respectively). The angles of N(1)–Zr–N(2) =

Table 1
Selected bond distances (Å) and angles (°) for complexes **2d** and **2g**

*Complex **2d***			
Zr–N(1)	2.238(3)	Zr–N(2)	2.236(3)
Zr–N(3)	2.187(3)	Zr–N(4)	2.259(3)
Zr–Cl(1)	2.4247(10)	Zr–Cl(2)	2.4176(10)
N(1)–C(1)	1.349(4)	N(2)–C(3)	1.327(4)
C(1)–C(2)	1.382(5)	C(2)–C(3)	1.399(5)
N(1)–Zr–N(2)	79.92(10)	N(3)–Zr–N(4)	80.25(11)
N(2)–Zr–N(3)	164.48(11)	Cl(1)–Zr–Cl(2)	91.08(4)
*Complex **2g***			
Zr–N(1)	2.229(4)	Zr–N(2)	2.272(4)
Zr–N(3)	2.229(3)	Zr–N(4)	2.259(4)
Zr–Cl(1)	2.4155(12)	Zr–Cl(2)	2.3983(15)
N(1)–C(1)	1.335(6)	N(2)–C(3)	1.334(5)
C(1)–C(2)	1.401(6)	C(2)–C(3)	1.395(5)
N(1)–Zr–N(2)	81.16(13)	N(3)–Zr–N(4)	80.57(14)
N(2)–Zr–N(4)	168.76(14)	Cl(1)–Zr–Cl(2)	89.26(5)

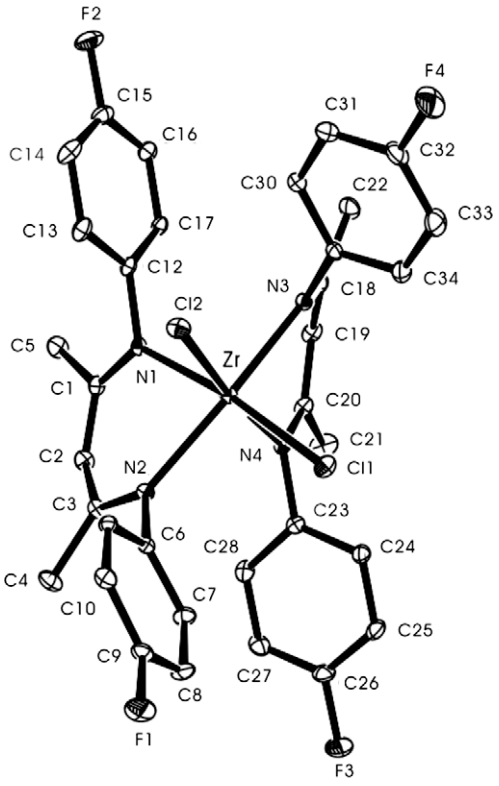

Fig. 1. ORTEP diagram of the molecular structure of **2d**. Thermal ellipsoids are drawn at the 50% probability level. Hydrogen atoms are omitted for clarity.

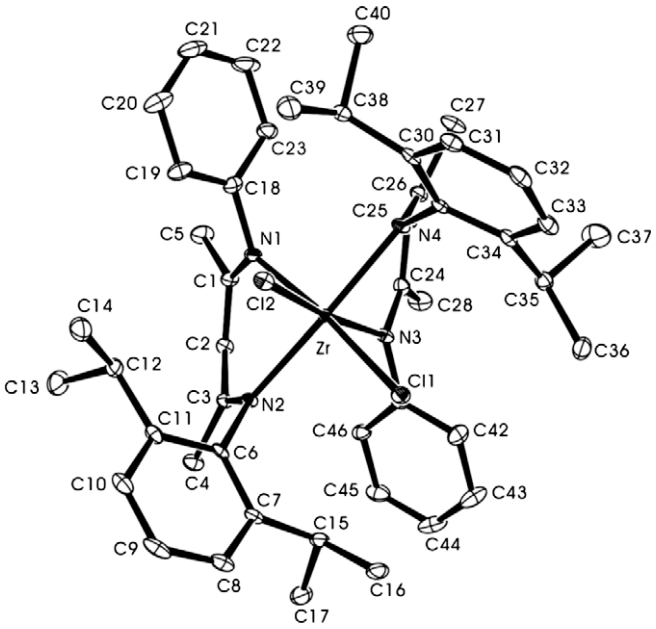

Fig. 2. ORTEP diagram of the molecular structure of **2g**. Thermal ellipsoids are drawn at the 50% probability level. Hydrogen atoms are omitted for clarity.

81.16(13)° and N(3)–Zr–N(4) = 80.57(14)° deviate considerably from 90°. Although N(1) and N(3) locate at the *trans*-positions of two *cis*-chlorine atoms, Zr–N(2) and Zr–N(4) bond distances of 2.259(4) and 2.272(4) Å are slightly longer than Zr–N(1) (2.229(4)) and Zr–N(3) (2.229(3) Å), respectively, most likely induced by the bulkier steric hindrance of the two *ortho*-isopropyl groups at the same phenyl ring. The much larger angle of N(2)–Zr–N(4) (168.76(14)°) in comparison with those in the previously reported **2a** [28] and **2b** [31] (N(1)–Zr–N(3) = 160.4(1)°, N(2)–Zr–N(3) = 157.65(6)°, respectively) as well as that in **2d** (N(2)–Zr–N(3) = 164.48(11)°) can also be attributed to the introduction of two bulky *ortho*-isopropyls. The very close bond lengths of N(1)–C(1) (1.335(6) Å) and N(2)–C(3) (1.334(5) Å), as well as C(1)–C(2) (1.401(6) Å) and C(2)–C(3) (1.395(5) Å), indicate the multiple bond character and significant delocalization in these bonds. The zirconium atom in **2g** situated 0.9753 Å out of the ligand plane defined by N(1), C(1), C(2), C(3) and N(2), which is bigger than that observed in complex **2d** (*vide supra*). Therefore it is reasonable to consider that the more bulky of the *ortho*-substituents, the larger the deviation of zirconium center from the backbone plane will be induced.

2.3. Polymerization of ethylene by complexes **2a–d**, **f–i**/MAO systems

β-Diketiminate zirconium complexes **2a–d**, **f–i** were effective for the polymerization of ethylene under different conditions with excess methylaluminoxane (MAO) as cocatalyst. The polymerization results are summarized in Tables 2 and 3. For complexes **2a–d** and **f** with symmetrical β-diketiminate ligand, the electronic nature of the *para*-substituents at the aromatic rings exerted great influence on the polymerization of ethylene. The catalytic activity for ethylene polymerization at 50 °C and 1.0 MPa increased in the order of **2d** (*p*-F) < **2c** (*p*-Cl) < **2b** (*p*-CH_3) < **2a** (*p*-H) < **2f** (*p*-CF_3) (Fig. 3), complex **2f** exhibited the highest catalytic activity of 7.62×10^5 g PE/mol-Zr · h among them. These results indicated that the CF_3 substituents in **2f** improved significantly the catalytic activity, probably due to the increase of electrophilicity of metal center and so accelerating the coordination/insertion rate of ethylene monomer. This is accordant with the results of previously reported β-diketiminate group 4 complexes [28,42,43]. The lower activity of **2b** than **2a** indicated that increase of the electron-donating ability of the *para*-substituent was disadvantaged to the catalytic activity [43]. The electron-donating groups at the phenyl rings decrease the electrophilicity of the zirconium center through the chelating π-system of the ancillary ligand, obviously unfavorable for the coordination and insertion of the ethylene monomer. Based on this point of view, complexes **2c** and **2d** bearing electron-withdrawing *para*-chloro or fluoro substituent should display increased catalytic activity. Unexpectedly, the halogen atoms substituted **2c** and **2d** showed lower catalytic activities than the unsubstituted **2a**, and complex **2c** was slightly more active than **2d**. The influence of halogen substitution at the ancillary ligands on the polymerization performance of the corresponding metal catalysts for olefins has been investigated in some cases, but conflictive results are usually obtained. An increase of ethylene catalytic activity was observed for the mono(β-diiminato) titanium complex with *ortho*-fluoro substituent [37]. Yang et al. reported that *ansa*-metallocence group 4 complexes with *para*-fluoro substituted at phenyl group displayed lower ethylene catalytic activity than the unsubstituted congener [47]. It's obvious that the effect of halogen substitution on catalytic activity is significantly complicated. Generally, halogen atoms are considered to show electronegative characteristic, but the lone pair in *p*-orbital of halogen atom can also lead to an electron-donating conjugated effect via *p*-π bonding to its *para*- and *ortho*-positions at phenyl ring. Therefore, it seems that the lower activities of complexes **2c** and **2d** than

Table 2
The polymerization of ethylene with **2a–d**, **f**/MAO as catalytic systems[a]

Run	Complex	[Al]/[Zr]	Temp (°C)	Yield PE (g)	Activity[b] 10^5	M_η[c] 10^5 g mol^{-1}	M_w[d] 10^5 g mol^{-1}	M_w/M_n[d]	T_m[e] (°C)
1	**2a**	1000	50	0.6353	2.54	11.5			
2		1000	70	0.4575	1.83	4.14			
3		1000	90	0.3625	1.45	0.45			
4[d]		1000	70	0.1407	0.59	0.89[f]			
5		2000	50	1.2250	4.90	–[g]			
6	**2b**	1000	50	0.5224	2.08	2.62	3.34	3.05	
7		1000	70	0.4178	1.64	2.18			
8		1000	90	0.0504	0.20	0.84			
9		2000	50	1.0153	4.06	–[g]			
10	**2c**	500	50	0.0655	0.26	3.84			
11		1000	50	0.4604	1.84	>9.70[h]			136.2
12		1000	70	0.3651	1.46	>3.00[h]			
13		1000	90	0.3525	1.41	1.63			
14		2000	50	0.8525	3.41	–[g]			130.3
15		4000	50	0.1330	0.53	8.75			
16	**2d**	1000	30	0.2102	0.84	9.60			
17		1000	50	0.3514	1.40	–[g]			
18		1000	70	0.2908	1.16	–[g]			
19		1000	90	0.2425	0.97	–[g]			
20		2000	50	0.3453	1.38	3.73			
21	**2f**	1000	30	0.5925	2.37	7.24			
22		1000	50	1.1150	4.26	6.38			
23		1000	70	1.2801	5.12	4.85			
24		1000	90	0.7175	2.87	1.81			
25		2000	70	1.8151	7.62	4.12			
26		4000	70	0.4951	1.98	1.78			

[a] Conditions: in toluene, V = 25 mL, [Zr] = 2×10^{-4} mol/L, $P_{ethylene}$ = 1.0 MPa, t_p = 0.5 h.
[b] g PE/mol-Zr · h.
[c] Molecular weights were determined by intrinsic viscosity measurements.
[d] M_w and M_w/M_n were determined by GPC.
[e] Melting temperature was determined by DSC.
[f] $P_{ethylene}$ = 0.5 MPa.
[g] Polymer sample could not be dissolved in decahydronaphthalene at 135 °C.
[h] Obtained for decahydronaphthalene soluble fraction by intrinsic viscosity measurements.

Table 3
The polymerization of ethylene with **2g–i**/MAO, (BDI-**1j**)$_2$ZrCl$_2$/LiCl/MAO as catalytic systems[a]

Run	Complex	[Al]/[Zr]	Temp (°C)	Yield PE (g)	Activity[b]10^5	M_η[c]10^5 g mol^{-1}	M_w[d]10^5 g mol^{-1}	M_w/M_n[d]	T_m[e] (°C)
27	**2g**	1000	30	0.1244	0.50	17.7			
28		1000	50	0.4405	1.76	17.1	19.2	14.8	
29		1000	70	0.3451	1.38	6.45			
30		1000	90	0.1350	0.54	1.48			
31		2000	50	0.6725	2.69	6.23			
32	**2h**	1000	50	0.3650	1.46	–[f]			137.3
33		1000	70	0.2752	1.10	–[f]			
34		1000	90	0.2608	1.04	2.00			
35		2000	50	0.6011	2.40	–[f]			
36	**2i**	500	50	*Trace*					
37		1000	50	0.5203	2.08	6.67			
38		1000	70	0.4102	1.64	>1.89[g]			
39		1000	90	0.2725	1.09	1.14			
40		2000	50	0.7875	3.15	0.94			
41		4000	50	0.3923	1.57	0.95			
42	(BDI-**1j**)$_2$ZrCl$_2$/LiCl[h]	1000	50	0.5902	2.36	10.6			
43		1000	70	0.3804	1.52	2.37			
44		1000	90	0.1628	0.65	0.77			
45		2000	50	0.8900	3.56	6.75			

[a] Conditions: in toluene, V = 25 mL, [Zr] = 2 × 10^{-4} mol/L, $P_{ethylene}$ = 1.0 MPa, t_p = 0.5 h.
[b] g PE/mol-Zr · h.
[c] Molecular weights were determined by intrinsic viscosity measurements.
[d] M_w and M_w/M_n were determined by GPC.
[e] Melting temperature was determined by DSC.
[f] Polymer sample could not be dissolved in decahydronaphthalene at 135 °C.
[g] Obtained for decahydronaphthalene soluble fraction by intrinsic viscosity measurements.
[h] The quantity used to carry out the polymerization Runs of (BDI-**1j**)$_2$ZrCl$_2$ was dependent on the results of elemental analysis.

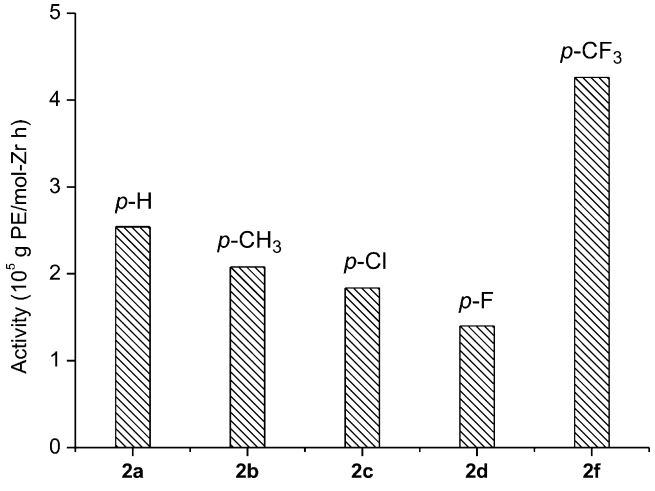

Fig. 3. Effect of different substitutents of zirconium complexes **2a**–**d** and **f** on the ethylene polymerization catalytic activity (polymerization conditions: in toluene, V = 25 mL, T_p = 50 °C, [Zr] = 2 × 10^{-4} mol/L, $P_{ethylene}$ = 1.0 MPa, t_p = 0.5 h, [Al]/[Zr] = 1000).

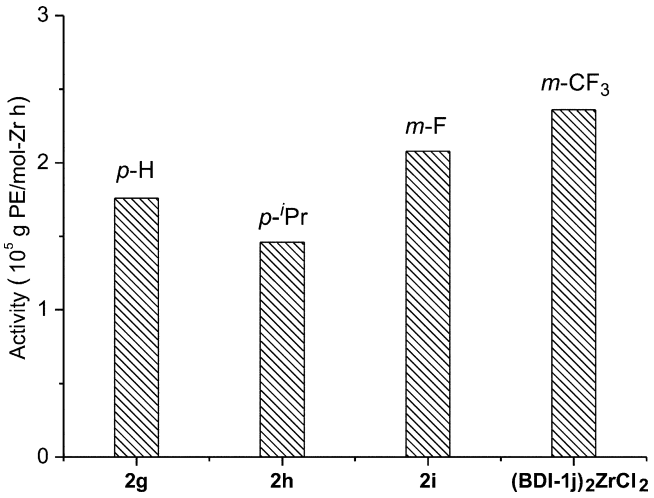

Fig. 4. Effect of different substitutents of zirconium complexes **2g**–**i** and (BDI-**1j**)$_2$ZrCl$_2$ on the ethylene polymerization catalytic activity (polymerization conditions: in toluene, V = 25 mL, T_p = 50 °C, [Zr] = 2 × 10^{-4} mol/L, $P_{ethylene}$ = 1.0 MPa, t_p = 0.5 h, [Al]/[Zr] = 1000).

the unsubstituted **2a** might be attributed to the electron-donating conjugated effect of fluorine and chlorine atoms.

As shown in Fig. 4, a comparison of the ethylene polymerization activities of complexes **2g–i** and (BDI-**1j**)$_2$ZrCl$_2$/LiCl [48] under the polymerization conditions of 50 °C and 1.0 MPa ethylene pressure revealed that the catalytic activity increased in the order of **2h** (*p*-^{i}Pr) < **2g** (*p*-H) < **2i** (*m*-F) < (BDI-**1j**)$_2$ZrCl$_2$/LiCl (*m*-CF$_3$). Despite of the introduction of *ortho*-isopropyls, the influence of the substituent at the other phenyl group on the catalytic activity was similar to that observed for the complexes **2a–d** and **f**. The introduction of electron-donating isopropyl group to the *para*-position of one of the aromatic rings in **2h** led to a decrease of activity. The *meta*-fluoro substituted complex **2i** exhibited higher activity than complex **2g**. Although an electron-donating conjugated effect by the *para*-fluoro substitution via *p*-π bonding was suggested to be responsible for the lower activity of complex **2d**, the *meta*-fluoro atom should show dominantly electron-withdrawing effect in **2g**, which increased significantly the electrophilicity of the metal center and led to an increase of catalytic activity than the unsubstituted analogue. Complex (BDI-**1j**)$_2$ZrCl$_2$ exhibited the highest catalytic activity among them due to the presence of strong electron-withdrawing *meta*-trifluoromethyl group. When compared with the complexes **2a–d** and **f**, zirconium complexes **2g–i** and (BDI-**1j**)$_2$ZrCl$_2$ showed slightly lower ethylene catalytic activity. It's evident that the bulky 2,6-diisopropyl groups at the aryl rings blocked the coordination sphere of the metal center to some extent and restrained the coordination/insertion of ethylene monomer [35].

As listed in Tables 2 and 3, the polymerization temperature had a remarkable effect on the catalytic behavior of these zirconium

complexes. When the polymerization temperature was raised from 30 to 90 °C, these complexes displayed the highest catalytic activity at about 50 °C except for complex **2f**, then the activity decreased gradually with the increase of temperature from 70 to 90 °C, which was most likely due to the thermal decomposition of the active species. Complex **2f** showed the highest catalytic activity at 70 °C (Run 23). It should be noticed that complexes **2c**, **2f** and **2h** could retain comparatively satisfactory activities even at 90 °C (Runs 13, 24 and 34). Compared with the titanium analogues [37,42,43], which reached the maximal values of catalytic activities at about 25 °C within the studied temperature range of 0–50 °C, these zirconium catalysts exhibited more excellent thermal stability. Sufficient activity at high polymerization temperature should be important especially with regard to the industrial application aspects, because performing a solution polymerization at high-temperature can reduce the viscosity of reaction mixture, leading to better mass transportation and temperature control.

The effect of ethylene pressure on polymerization behavior of these β-diketiminate zirconium complexes was also studied. For complex **2a**, the decrease of catalytic activity (from 1.83 to 0.59×10^5 g PE/mol-Zr · h) and molecular weight (from 4.14 to 0.89×10^5 g/mol) of the produced polymers was significant (Run 2 versus 4) when the ethylene pressure decreased from 1.0 to 0.5 MPa. The lower ethylene pressure resulted in the reduction of the monomer concentration in solution, which was the main reason for the decrease in the catalytic activity and molecular weight [47,49].

The amount of cocatalyst MAO always had significant influence on the catalytic performance of these complexes. In general, the catalytic activity increased with the enhancement of [Al]/[Zr] ratio from 1000 to 2000. Further increasing the [Al]/[Zr] ratio to 4000 led to the decrease of catalytic activities of **2c**, **2f** and **2i** (Runs 15, 26, 41). Probably the surface of active species was overlaid with the excess MAO, which led to the inactivity of catalysts. At lower [Al]/[Zr] ratio of 500, a sharp drop in activity was observed for complexes **2c** and **2i** (Runs 10 and 36), the small amount of MAO was not enough to activate the catalysts. Considerable influence of the amount of MAO on the molecular weights of produced polymers was also observed. In the cases of **2a**, **2b** and **2c**, when the [Al]/[Zr] ratio enhanced from 1000 to 2000 (Runs 5, 9 and 14), the molecular weight of produced polyethylenes increased considerably, which could not be determined by neither M_w using GPC nor viscosity average molecular weight based on $[\eta]$ due to the rather poor solubility in *o*-dichlorobenzene or decahydronaphthalene at 135 °C. The obtainment of ultra-high molecular weight polyethylenes (UHMWPE) is therefore suggested [50,51].

The molecular weights of our polyethylene samples are considerably higher than those afforded by other β-diketiminate group 4 complexes ($M_w = 1 \sim 9 \times 10^5$ g/mol) in published literatures under similar conditions [28,37,42,43]. The production of UHMWPE probably resulted from the significantly faster chain propagation rate than β-hydride elimination or chain transfer reaction. These polymers could represent some of those possessing highest molecular weight encountered in homogenous olefin polymerization catalysts, including the group 4 metallocene catalysts [52–55].

Though showing slightly lower activity than **2a**–**d** and **f**, complexes **2g**–**i** exhibited different catalytic performance compared with the smaller congeners. Complex **2g** could produce polyethylene of high molecular weight (M_η: 17.1×10^5 g/mol), which is even higher than that afforded by **2a** (M_η: 11.5×10^5 g/mol) (Run 1 versus 28) under same conditions. It is noteworthy that complex **2h** also produced extremely high molecular weight polyethylene (Runs 32, 33 and 35), which hardly dissolves in decahydronaphthalene under the intrinsic viscosity measurement conditions. This increase of molecular weight was possibly due to a decrease in the rate of β-hydride elimination or chain transfer reaction, which was a consequence of the increased steric congestion around the active metal center.

Complex **2b** produced polymers with molecular weight distribution (MWD) of 3.05 (Run 6), which was comparable to the previous report of **2a** (MWD = 2.70) [28] as well as titanium analogues [37,43] and indicated the single-site catalytic property under these conditions. In addition, high-temperature ^{13}C NMR analysis of the polyethylene produced by **2b** (Run 6) indicates that the polymer

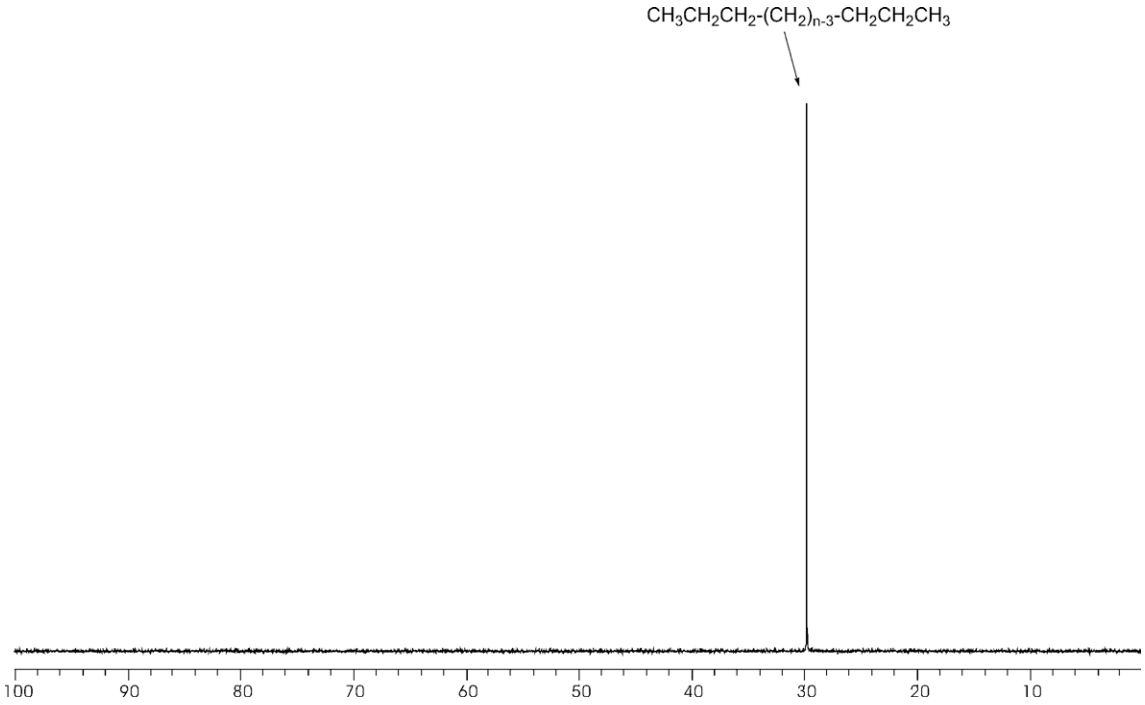

Fig. 5. ^{13}C NMR spectrum of polyethylene (sample of Run 6) prepared with complex **2b** (100 MHz, 1,2-dichlorobenzene-d_4, 100 °C).

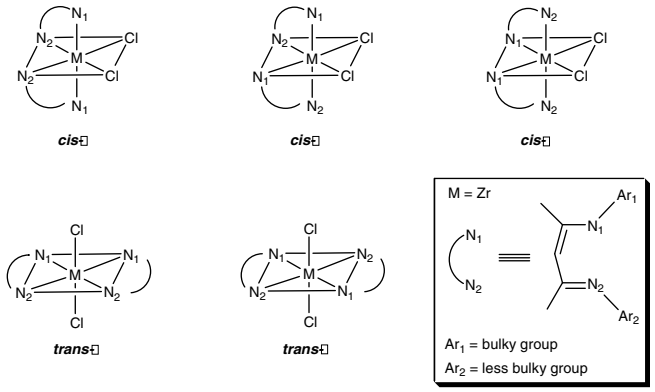

Scheme 3. The possible isomers of metal complex with general formula of $[N_1,N_2]_2MCl_2$.

possesses linear structure with virtually no branching (Fig. 5). Melting temperature measured by DSC also proves the polymer as typical linear polyethylene (Runs 11 and 14).

It was expected that complexes **2g–i** bearing unsymmetrical ligand structure with the bulky *ortho*-isopropyls at one of the two phenyls displayed different catalytic property from **2a–d** and **f**. Complex **2g** produced polyethylenes with very broad MWD (14.8) (Run 28). Although the X-ray diffraction measurement (Fig. 2) and ^{1}H NMR data suggested the unique structure of **2g** where it adopted the configuration of *cis*-I with two N2 in the *cis*-positions and two N1 in the *trans*-positions in order to reduce the steric congestion of the ligand (Scheme 3), the formation of polyethylenes with broad MWD indicated the existence of multi active species under the polymerization conditions, which was also suggested by the authors of previously reported group 4 metal diiminato complexes producing broad MWD polyethylenes [30,37,39]. As depicted in Scheme 3, chelating complexes of the form $[N_1,N_2]_2MCl_2$ potentially possess five isomers besides the common *cis*-I isomer raised from the versatile coordination modes of ligands in an octahederal geometry. Minor isomers are sometimes observable accompanied with the major *cis*-N2, *trans*-N1, *cis*-Cl isomer by NMR spectroscopy, even though single crystals of *cis*-N2, *trans*-N1, *cis*-Cl isomer characterized by X-ray diffraction were used for the NMR experiment [44]. Li's group [36] revealed the existence of isomers of β-diketiminate titanium complex by ^{19}F NMR spectroscopy. Recently Fujita and collaborators [44] found that bis(phenoxy-imine)zirconium complex with bulky substituent at the phenoxy *ortho*-position possessed at least two isomers by ^{15}N NMR, and this complex could afford polyethylenes with multimodal MWD (2–24). Therefore, it is possible that the highly fluxional character of the complex is connected with the multimodal MWD of polymers. Here, we tentatively regarded that the production of broad MWD polyethylene was relevant to the introduction of bulk unsymmetrical auxiliary ligand to the center metal, which promoted the formation of multi active species under the polymerization conditions. Furthermore, the ^{13}C NMR spectrum reveals that similar to that afforded by complex **2b** polyethylenes produced by **2g** are linear. The DSC result of polymer sample by complex **2i** also shows the character of linear polyethylene (Run 32).

3. Conclusions

A series of zirconium complexes bearing symmetrical or unsymmetrical β-diketiminate ligands were synthesized, among which the octahedral geometric structure of complexes **2d** and **2g** were confirmed by X-ray diffraction study. Complexes **2g–i** probably represented the first examples that the zirconium complexes bearing unsymmetrical β-diketiminate ligand. The ethylene polymerization behavior of these complexes were investigated. Experimental results showed that the substitutents at the *N*-aromatic rings displayed an important role in the catalytic performance of these β-diketiminate zirconium complexes. *Para*-trifluoromethyl substituted **2f** showed the highest catalytic activity among them due to the strong electron-withdrawing effect of CF_3. UHMWPEs could be produced by **2a–d** possibly ascribed to the considerably faster rate of chain propagation than β-hydride elimination or chain transfer reaction. Complexes **2g–i** and (BDI-**1j**)$_2$ZrCl_2/LiCl could afford polyethylenes with broad MWD (14.8), which most likely resulted from the introduction of bulkily unsymmetrical β-diketiminate ligands. It was noteworthy that these zirconium complexes were capable of controlling the molecular weights of resulted polymers (M_η: 0.45–17.7 × 10^5 or even higher) as well as the MWD of obtained polyethylenes from 3.05 to 14.8 by changing the ligand structure and the polymerization conditions.

4. Experimental

4.1. General

All manipulations were carried out under a dry argon atmosphere using standard Schlenk techniques or a glove-box unless otherwise indicated. Toluene and diethyl ether was refluxed and distilled over sodium benzophenone ketyl prior to use. Chloroform-*d* and 1-hexene were dried over calcium hydride under argon prior to use. *n*-BuLi (2.5 M in *n*-hexane) were purchased from Chemetall. Methylaluminoxane (MAO) of 1.53 M in toluene was purchased from Witco. ^{1}H NMR spectra were recorded on Bruker AVANCE-500 spectrometers with $CDCl_3$ as solvent. Chemical shifts for ^{1}H NMR spectra were referenced internally using the residual solvent resonances and reported relative to tetramethylsilane (TMS). Melting points were determined in sealed glass capillaries under argon and reported without correction. Elemental analyses were carried out on an EA-1106 type analyzer. ESI-MS spectra were recorded on a Micromass LCT mass instrument. Polymeric grade ethylene was directly used for polymerization without further purification. $ZrCl_4 \cdot 2THF$ [56], β-diketimines **1c–g** and **k** [45], complexes **2a** [28] and **2b** [31] were synthesized according to the published procedures. All other reagents were obtained from standard commercial vendors and used as received.

^{13}C NMR spectra of polymers were recorded on a Bruker AVANCE-500 spectrometer in 1,2-dichlorobenzene-d_4 at 100 °C. The intrinsic viscosities of polyethylenes (PE) were measured with an Ubbelohde viscometer in decahydronaphthalene at 135 °C. The viscosity average molecular weights of PEs were calculated according to the equation: $[\eta]$ (dL/g) = 6.77 × 10^{-4} $M_\eta^{0.67}$ [57]. The gel permeation chromatography (GPC) performed on a Waters 150 ALC/GPC system in a 1,2-dichlorobenzene solution at 135 °C was used to determine the weight-average molecular weights (M_w) and the molecular weight distributions (M_w/M_n) of the polymers. Differential scanning calorimetry (DSC) was performed on a Universal V2.3C TA instrument. The polymer sample was first equilibrated at 0 °C and then heated to 200 °C at a rate of 10 °C/min to remove thermal history, After being cooled to 0 °C at a rate of 10 °C/min, the second heating scan was run from 0 to 200 °C at a rate of 10 °C/min, and the data are reported according to the second heating scan.

4.2. Synthesis of ligands and complexes

4.2.1. Synthesis of 2-(2,6-diisopropylphenyl)amino-4-(4-isopropylphenyl)imino-2-pentene (*1h*)

The synthetic procedure was similar to that of β-diketimine **1g** [45]. 9.510 g (50.00 mmol) of *para*-toluenesulfonic acid

monohydrate, 6.761 g (50.00 mmol) of 4-isopropylaniline, 12.97 g (50.00 mmol) of 4-(2,6-diisopropylphenyl)amino-3-penten-2-one, and 80 mL of toluene were combined in a round bottomed flask. A Dean–Stark apparatus was attached and the mixture was heated at reflux for 24 h to remove the water. The reaction mixture was cooled to r.t. and all the volatiles were removed under reduced pressure to give a yellow solid. The solid was treated with diethyl ether (100 mL), water (100 mL) and sodium carbonate (10.60 g, 100 mmol), and the obtained mixture was kept stirring. After complete dissolution, the aqueous phase was separated and extracted with diethyl ether. The combined organic phase was dried over $MgSO_4$ and rotary evaporated to dryness under reduced pressure to afford a yellow solid. Yellow crystals (12.80 g, 68%) were obtained after recrystallization from methanol. M.p. 85–86 °C. ^{1}H NMR (500 MHz, $CDCl_3$, 25 °C): δ 1.13 (d, ^3J = 6.8 Hz, 6H, –CH(CH_3)$_2$), 1.21 (d, ^3J = 6.8 Hz, 6H, –CH(CH_3)$_2$), 1.22 (d, ^3J = 6.8 Hz, 6H, –CH(CH_3)$_2$), 1.69 (s, 3H, CH_3), 2.06 (s, 3H, CH_3), 2.86 (sept, ^3J = 6.8 Hz, 1H, –C*H*(CH$_3$)$_2$), 2.98 (sept, ^3J = 6.8 Hz, 2H, –C*H*(CH$_3$)$_2$), 4.85 (s, 1H, γ-C*H*), 6.89 (d, 2H, ^3J = 9.0 Hz, *o*-Ar-*H*), 7.07–7.13 (m, 5H, *m*-, *p*-Ar-*H*), 12.70 (br s, 1H, N*H*). ^{13}C NMR (100 MHz, $CDCl_3$, 25 °C): δ 19.6 (C*Me*), 20.1 (C*Me*), 21.6 (CH*Me*$_2$), 23.0 (CH*Me*$_2$), 27.1 (C*H*Me$_2$), 32.4 (C*H*Me$_2$), 94.4 (C*H*), 121.6 (Ar-*C*), 121.8 (Ar-*C*), 123.0 (Ar-*C*), 126.0 (Ar-*C*), 139.3 (Ar-*C*), 140.4 (Ar-*C*), 142.1 (Ar-*C*), 142.6 (Ar-*C*), 155.4 (N*C*Me), 162.2 (N*C*Me). Anal. Calc. for $C_{26}H_{36}N_2$: C, 82.93; H, 9.64; N, 7.44. Found: C, 82.94; H, 9.65; N, 7.40%.

4.2.2. Synthesis of 2-(2,6-diisopropylphenyl)amino-4-(3-fluorophenyl)imino-2-pentene (*1i*)

β-Diketimine **1i** was synthesized by the same procedure of **1h**. 9.510 g (50.00 mmol) of *para*-toluenesulfonic acid monohydrate, 5.561 g (50.00 mmol) of 3-fluoroaniline and 12.97 g (50.00 mmol) of 4-(2,6-diisopropylphenyl)amino-3-penten-2-one were used to give 12.34 g (70%) of light yellow crystals. M.p. 90–91 °C. ^{1}H NMR (500 MHz, $CDCl_3$, 25 °C): δ 1.12 (d, ^3J = 6.9 Hz, 6H, –CH(CH_3)$_2$), 1.20 (d, ^3J = 6.9 Hz, 6H, –CH(CH_3)$_2$), 1.67 (s, 3H, CH_3), 2.03 (s, 3H, CH_3), 3.00 (sept, ^3J = 6.9 Hz, 2H, –C*H*(CH$_3$)$_2$), 4.87 (s, 1H, γ-C*H*), 6.58–6.69 (m, 3H, *o*-, *p*-Ar-*H*), 7.11–7.19 (m, 4H, *m*-, *p*-Ar-*H*), 12.54 (br s, 1H, N*H*). ^{13}C NMR (100 MHz, $CDCl_3$, 25 °C): δ 19.1 (C*Me*), 19.8 (C*Me*), 21.4 (CH*Me*$_2$), 23.2 (CH*Me*$_2$), 27.2 (C*H*Me$_2$), 94.8 (C*H*), 107.8 (Ar-*C*), 107.9 (Ar-*C*), 108.0 (Ar-*C*), 116.5 (Ar-*C*), 121.9 (Ar-*C*), 124.3 (Ar-*C*), 128.6 (Ar-*C*), 138.9 (Ar-*C*), 141.3 (Ar-*C*), 147.3 (Ar-*C*), 158.4 (Ar-*C*), 160.0 (Ar-*C*), 161.2 (N*C*Me), 163.2 (N*C*Me). Anal. Calc. for $C_{23}H_{29}FN_2$: C, 78.37; H, 8.29; N, 7.95. Found: C, 77.90; H, 8.36; N, 7.81%.

4.2.3. Synthesis of 2-(2,6-diisopropylphenyl)amino-4-(3-trifluoromethylphenyl)imino-2-pentene (*1j*)

β-Diketimine **1j** was synthesized by the same procedure of **1h**. 9.510 g (50.00 mmol) of *para*-toluenesulfonic acid monohydrate, 8.056 g (50.00 mmol) of 3-trifluoromethylaniline and 12.97 g (50.00 mmol) of 4-(2,6-diisopropylphenyl)amino-3-penten-2-one were used to give 14.69 g (73%) of yellow crystals. M.p. 85.5–87.5 °C. ^{1}H NMR (500 MHz, $CDCl_3$, 25 °C): δ 1.24 (d, ^3J = 6.9 Hz, 6H, –CH(CH_3)$_2$), 1.33 (d, ^3J = 6.9 Hz, 6H, –CH(CH_3)$_2$), 1.80 (s, 3H, CH_3), 2.12 (s, 3H, CH_3), 3.15 (sept, ^3J = 6.9 Hz, 2H, –C*H*(CH$_3$)$_2$), 5.02 (s, 1H, γ-C*H*), 7.13 (d, ^3J = 7.8 Hz, 1H, *o*-Ar-*H*), 7.22 (s, 1H, *o*-Ar-*H*), 7.24–7.30 (m, 3H, *m*-, *p*-Ar-*H*), 7.34 (d, ^3J = 7.8 Hz, 1H, *p*-Ar-*H*), 7.45 (t, ^3J = 7.8 Hz, 1H, *m*-Ar-*H*), 12.58 (br s, 1H, N*H*). ^{13}C NMR (100 MHz, $CDCl_3$, 25 °C): δ 19.3 (C*Me*), 19.8 (C*Me*), 21.4 (CH*Me*$_2$), 23.3 (CH*Me*$_2$), 27.3 (C*H*Me$_2$), 94.8 (C*H*), 117.4 (Ar-*C*), 117.9 (Ar-*C*), 122.0 (Ar-*C*), 123.3 (q, $^1J_{C\text{-}F}$ = 270.3 Hz, CF_3), 124.0 (Ar-*C*), 124.8 (Ar-*C*), 128.1 (Ar-*C*), 130.0 (q, $^2J_{C\text{-}C\text{-}F}$ = 32.2 Hz, Ar-*C*), 137.9 (Ar-*C*), 142.1 (Ar-*C*), 146.9 (Ar-*C*), 159.4 (N*C*Me), 159.9 (N*C*Me). Anal. Calc. for $C_{24}H_{29}F_3N_2$: C, 71.62; H, 7.26; N, 6.96. Found: C, 71.82; H, 7.42; N, 6.83%.

4.2.4. Synthesis of complex *2c*

To a solution of ligand **1c** (0.798 g, 2.50 mmol) in 10 mL of toluene was added dropwise *n*-BuLi (2.5 M, 1.0 mL, 2.5 mmol) in *n*-hexane at −78 °C. The mixture was stirred and slowly allowed to warm to ambient temperature. After being stirred for additional 12 h, the solution was added dropwise to a stirred suspension of $ZrCl_4 \cdot 2$THF (0.472 g, 1.25 mmol) in toluene at −78 °C. The reaction mixture was allowed to warm to room temperature and stirred overnight. Then the solvent was removed under reduced pressure and the obtained yellow solid was extracted several times with hot toluene. The filtrates were combined and was concentrated to ca. 40 mL under vacuum and deposited at −20 °C overnight. Precipitate was isolated by filtration and dried in vacuum to give 0.448 g (45%) of yellow crystals. M.p. 180–185 °C (dec). ^{1}H NMR (500 MHz, $CDCl_3$, 25 °C): δ 1.65 (s, 12H, CH_3), 5.42 (s, 2H, γ-C*H*), 6.77–7.24 (m, 16H, Ar-*H*). ESI-MS (*m/s*): 798 (M^+). Anal. Calc. for $C_{34}H_{30}N_4Cl_6Zr$: C, 51.14; H, 3.79; N, 7.02. Found: C, 51.53; H, 3.91; N, 6.66%.

4.2.5. Synthesis of complex *2d*

Complex **2d** was synthesized using the same procedure as **2c**. 0.716 g (2.50 mmol) of β-diketimine **1d**, 1.0 mL of *n*-BuLi (2.5 M, 2.50 mmol) in *n*-hexane, and 0.472 g (1.25 mmol) of $ZrCl_4 \cdot 2$THF were used to give 0.467 g (51%) of orange yellow crystals. M.p. 189–192 °C (dec). ^{1}H NMR (500 MHz, $CDCl_3$, 25 °C): δ 1.65 (s, 12H, CH_3), 5.43 (s, 2H, γ-C*H*), 6.82–7.00 (m, 16H, Ar-*H*). ESI-MS (*m/s*): 732 (M^+). Anal. Calc. for $C_{34}H_{30}N_4Cl_2F_4Zr$: C, 55.73; H, 4.13; N, 7.65. Found: C, 55.61; H, 4.15; N, 7.66%.

4.2.6. Synthesis of complex *2f*

To a solution of ligand **1f** (0.965 g, 2.50 mmol) in 10 mL of diethyl ether was added dropwise *n*-BuLi (2.5 M, 1.0 mL, 2.50 mmol) in *n*-hexane at −78 °C. The mixture was stirred and slowly allowed to warm to ambient temperature. After being stirred for additional 12 h, the solution was added dropwise to a stirred suspension of $ZrCl_4 \cdot 2$THF (0.472 g, 1.25 mmol) in 10 mL of diethyl ether at −78 °C. The reaction mixture was allowed to warm to room temperature and stirred overnight. Then the mixture was dried under reduced pressure and the obtained yellow solid was extracted with 20 mL diethyl ether. The filtrate was concentrated to ca. 6 mL under vacuum and deposited at −20 °C overnight. Precipitate was isolated by filtration and dried in vacuum to afford 0.757 g (64%) of orange yellow crystals. M.p. 135–140 °C (dec). ^{1}H NMR (500 MHz, $CDCl_3$, 25 °C): δ 1.69 (s, 12H, CH_3), 5.52 (s, 2H, γ-C*H*), 6.94–7.05 (m, 8H, *o*-Ar-*H*), 7.54 (d, ^3J = 8.1 Hz, 8H, m-Ar-*H*). ESI-MS (*m/s*): 932 (M^+). Anal. Calc. for $C_{38}H_{30}Cl_2F_{12}N_4Zr$: C, 48.93; H, 3.24; N, 6.01. Found: C, 48.56; H, 3.47; N, 5.72%.

4.2.7. Synthesis of complex *2g*

Complex **2g** was synthesized using the same procedure of **2c**. 0.836 g (2.50 mmol) of β-diketimine **1g**, 1.0 mL of *n*-BuLi (2.5 M, 2.50 mmol) in *n*-hexane, and 0.472 g (1.25 mmol) of $ZrCl_4 \cdot 2$THF were used to give 0.571 g (55%) of orange yellow crystals. M.p. 108–110 °C (dec). ^{1}H NMR (500 MHz, $CDCl_3$, 25 °C): δ 0.70 (d, ^3J = 6.5 Hz, 6H, –CH(CH_3)$_2$), 0.86 (d, ^3J = 6.5 Hz, 6H, –CH(CH_3)$_2$), 0.93 (d, ^3J = 6.5 Hz, 6H, –CH(CH_3)$_2$), 1.27 (d, ^3J = 6.5 Hz, 6H, –CH(CH_3)$_2$), 1.89 (s, 6H, CH_3), 1.91 (s, 6H, CH_3), 3.00 (sept, ^3J = 6.5 Hz, 4H, –C*H*(CH$_3$)$_2$), 5.86 (s, 2H, γ-C*H*), 6.92–7.28 (m, 16H, Ar-*H*). ESI-MS (*m/s*): 828 (M^+). Anal. Calc. for $C_{46}H_{58}Cl_2N_4Zr \cdot 0.7(C_7H_8)$: C, 68.49; H, 7.17; N, 6.25. Found: C, 68.57; H, 7.71; N, 5.81%.

4.2.8. Synthesis of complex *2h*

Complex **2h** was synthesized using the same procedure of **2c**. 0.942 g (2.50 mmol) of β-diketimine **1h**, 1.0 mL of *n*-BuLi (2.5 M, 2.50 mmol) in *n*-hexane, and 0.472 g (1.25 mmol) of $ZrCl_4 \cdot 2$THF

were used to give 0.537 g (47%) of orange yellow crystals. M.p. 121.5–123.5 °C. ^{1}H NMR (500 MHz, $CDCl_3$, 25 °C): δ 0.72 (d, ^3J = 6.5 Hz, 6H, –CH(CH_3)$_2$), 0.84 (d, ^3J = 6.5 Hz, 6H, –CH(CH_3)$_2$), 0.92 (d, ^3J = 6.5 Hz, 6H, –CH(CH_3)$_2$), 1.28–1.32 (m, 18H, –CH(CH_3)$_2$), 1.86 (s, 6H, CH_3), 1.93 (s, 6H, CH_3), 2.91–3.00 (m, 6H, –CH(CH_3)$_2$), 5.84 (s, 2H, γ-CH), 6.97–7.18 (m, 14H, Ar-H). ESI-MS (*m/s*): 912 (M^+). Anal. Calc. for $C_{52}H_{70}Cl_2N_4Zr$: C, 68.39; H, 7.73; N, 6.13. Found: C, 67.91; H, 8.01; N, 5.58%.

4.2.9. Synthesis of complex **2i**

Complex **2i** was synthesized using the same procedure of **2c**. 0.881 g (2.5 mmol) of β-diketimine **1i**, 1.0 mL of *n*-BuLi (2.5 M, 2.5 mmol) in *n*-hexane, and 0.472 g (1.25 mmol) of $ZrCl_4 \cdot 2THF$ were used to obtain 0.530 g (49%) of orange yellow crystals. M.p. 134–137 °C (dec). ^{1}H NMR (500 MHz, $CDCl_3$, 25 °C): δ 0.77 (d, ^3J = 6.5 Hz, 6H, –CH(CH_3)$_2$), 0.84 (d, ^3J = 6.5 Hz, 6H, –CH(CH_3)$_2$), 0.95 (d, ^3J = 6.5 Hz, 6H, –CH(CH_3)$_2$), 1.34 (d, ^3J = 6.5 Hz, 6H, –CH(CH_3)$_2$), 1.90 (s, 6H, CH_3), 1.92 (s, 6H, CH_3), 2.91 (sept, ^3J = 6.5 Hz, 4H, –CH(CH_3)$_2$), 5.86 (s, 2H, γ-CH), 6.92–7.31 (m, 14H, Ar-H). ESI-MS (*m/s*): 864 (M^+). Anal. Calc. for $C_{46}H_{56}Cl_2F_2N_4Zr$: C, 63.87; H, 6.52, N, 6.48. Found: C, 63.12; H, 6.63; N, 6.16%.

4.2.10. Generation of complex (BDI-**1j**)$_2ZrCl_2$

The mixture of complex (BDI-**1j**)$_2ZrCl_2$ and LiCl was prepared as the followed procedure. To a solution of ligand **1j** (1.006 g, 2.50 mmol) in 10 mL of toluene was added dropwise 1.0 mL of *n*-BuLi (2.5 M, 2.50 mmol) in *n*-hexane at −78 °C. The mixture was stirred and slowly allowed to warm to ambient temperature. After being stirred for additional 12 h, the solution was added dropwise to a stirred suspension of $ZrCl_4 \cdot 2THF$ (0.472 g, 1.25 mmol) in 10 mL of toluene at −78 °C. The reaction mixture was allowed to warm to room temperature and stirred overnight. The mixture was dried under reduced pressure and washed with toluene twice. Then the obtained 0.916 g of yellow solid was dried in vacuum. ^{1}H NMR (500 MHz, $CDCl_3$, 25 °C): δ 0.80 (d, ^3J = 6.4 Hz, 6H, –CH(CH_3)$_2$), 0.96 (d, ^3J = 6.4 Hz, 6H, –CH(CH_3)$_2$), 1.02 (d, ^3J = 6.4 Hz, 6H, –CH(CH_3)$_2$), 1.43 (d, ^3J = 6.4 Hz, 6H, –CH(CH_3)$_2$), 2.01 (s, 6H, CH_3), 2.03 (s, 6H, CH_3), 3.13 (m, 4H, –CH(CH_3)$_2$), 6.04 (s, 2H, γ-CH), 7.12–7.47 (m, 14H, Ar-H). Anal. Calc. for $C_{48}H_{56}Cl_2F_6N_4Zr \cdot 2LiCl$: C, 54.91; H, 5.38; N, 5.34. Found: C, 50.51; H, 5.50; N, 4.82%.

4.3. X-ray diffraction measurements

The crystallographic data for complexes **2d** and **2g** were collected on a Bruker AXSD8 diffractometer with graphite-monochromated Mo Kα (λ = 0.71073 Å) radiation. All data were collected at 20 °C using the ω-scan techniques. Details of the crystal data and structure refinements are summarized in Table 4. The structures of **2d** and **2g** were solved by direct methods and refined using Fourier techniques. An absorption correction based on SADABS was applied [58]. All non-hydrogen atoms were refined by full-matrix least-squares on F^2 using the SHELXTL program package [59]. Hydrogen atoms were located and refined by the geometry method. The cell refinement, data collection, and reduction were done by Bruker SAINT [60]. The structure solution and refinement were performed by SHELXTL-97 [61] and SHELXTL-97 [62], respectively.

4.4. Polymerization procedure

Ethylene polymerization was carried out in a 100 mL autoclave equipped with a magnetic stirrer. The autoclave was heated at 100 °C under vacuum for 30 min and then cooled to the desired temperature by immerging into a thermostatically heated bath, then filled with ethylene. Proper amount of MAO solution and toluene were added to the autoclave and was filled with ethylene for 15 min at the reaction temperature. After proper amount of toluene solution of zirconium complex was injected to the reactor, ethylene at desired pressure was introduced to start the polymerization. The reaction mixture was stirred vigorously for a certain time and the ethylene pressure in the autoclave was slowly vented. Then 10 mL of ethanol was added to terminate the polymerization. The resulting mixture was poured into 3% HCl in ethanol (50 mL). The polymer was collected by filtration, washed with ethanol (30 mL × 2), and then dried for 16 h in a vacuum oven at 60 °C to constant weight.

Table 4
Crystal data and structure refinement details for **2d** and **2g**

	2d	**2g**
Empirical formula	$C_{34}H_{30}Cl_2F_4N_4Zr$	$C_{46}H_{58}Cl_2N_4Zr$
Formula weight	732.74	829.08
Temp (K)	293(2)	293(2)
Wavelength (Å)	0.71073	0.71073
Crystal size (mm^3)	0.400 × 0.212 × 0.056	0.311 × 0.211 × 0.047
Crystal system	Monoclinic	Triclinic
Space group	$P2(1)/n$	$P\bar{1}$
a (Å)	12.5931(8)	8.8115(12)
b (Å)	15.9559(10)	12.4202(17)
c (Å)	17.1990(11)	21.341(3)
α (°)	90.00	73.676
β (°)	111.3190(10)	82.271
γ (°)	90.00	78.469
Volume (Å^3)	3219.4(4)	2188.6(5)
Z	4	2
Calc. density (Mg/m^3)	1.512	1.258
Absorption coefficient (mm^{-1})	0.562	0.408
$F(000)$	1488	872
θ range for data collection (°)	1.74–27.00	1.76–25.50
limiting indices	$-16 \leqslant h \leqslant 15$, $-20 \leqslant k \leqslant 20$, $-21 \leqslant l \leqslant 18$	$-6 \leqslant h \leqslant 10$, $-15 \leqslant k \leqslant 15$, $-25 \leqslant l \leqslant 25$
Reflection collected/unique	18748/6964 [$R_{(int)}$ = 0.0697]	11439/8016 [$R_{(int)}$ = 0.0698]
Max. and min. transmission	1.00000 and 0.88551	1.00000 and 0.77199
Data/restrains/parameters	6964/0/410	8016/0/490
Goodness-of-fit on F^2	0.869	0.879
Final R indices [I > 2σ(I)]	R_1 = 0.0521, wR_2 = 0.0830	R_1 = 0.0570, wR_2 = 0.0795
R Indices (all data)	R_1 = 0.0913, wR_2 = 0.0943	R_1 = 0.1257, wR_2 = 0.0943
Largest difference in peak/hole (e Å^{-3})	0.482 and –0.483	0.554 and –0.660

Acknowledgements

This work is subsidized by the National Basic Research Program of China (2005CB623801), National Natural Science Foundation of China (NNSFC, 20604009, 20774027), the Program for New Century Excellent Talents in University (for H. Ma, NCET-06-0413), Shanghai Rising-Star Program (06QA14014) and the Scientific Research Foundation for the Returned Overseas Chinese Scholars (SRF for ROCS, SEM). All the financial supports are gratefully acknowledged. The authors also thank the very kind donation of a glove-box by the AvH foundation.

Appendix A. Supplementary material

CCDC 689400 and 689401 contain the supplementary crystallographic data for **2d** and **2g**. These data can be obtained free of charge from the Cambridge Crystallographic Data Centre via www.ccdc.cam.ac.uk/data_request/cif. Supplementary data associated with this article can be found, in the online version, at doi:10.1016/j.jorganchem.2008.08.024.

References

[1] L.C. Wang, M.K. Harvey, J.C. Ng, U. Scheunemann, J. Power Sources 73 (1998) 74–77.
[2] J.C. Liu, US Patent 6635728, 2003.
[3] S. Rastogi, P. Lemstra, WO Patent 9835818, 1998.
[4] H. Knuuttila, P. Sormnnenm, WO Patent 9507305, 1995.
[5] P. Brant, J. Canich, US Patent 5444145, 1995.
[6] M.S. Weiser, M. Wesolek, R. Mulhaupt, J. Organomet. Chem. 691 (2006) 2945–2952.
[7] Y.-X. Chen, T.J. Marks, Organometallics 16 (1997) 3649–3657.
[8] M.E. Bluhm, C. Folli, D. Pufky, M. Kroger, O. Walter, M. Doring, Organometallics 24 (2005) 4139–4152.
[9] J.P. George, M.B. Britovsek, V.C. Gibson, B.S. Kimberley, P.J. Maddox, S. Mastroianni, S.J. McTavish, C. Redshaw, G.A. Solan, S. Stro1mberg, A.D. Williams, J. Am. Chem. Soc. 121 (1999) 8728–8740.
[10] G. Baruzzi, C.J. Schwvierien, Eur Patent 0942011, 1999.
[11] V.C. Gibson, S.K. Spitzmesser, Chem. Rev. 103 (2003) 283–315.
[12] D.V. Vitanova, F. Hampel, K.C. Hultzsch, Dalton Trans. 5 (2005) 1565–1566.
[13] D.V. Vitanova, F. Hampel, K.C. Hultzsch, J. Organomet. Chem. 690 (2005) 5182–5197.
[14] M.F. Pilz, C. Limberg, B. Ziemer, J. Org. Chem. 71 (2006) 4559–4564.
[15] T.J. Hebden, W.W. Brennessel, C.J. Flaschenriem, P.L. Holland, Dalton Trans. (2006) 3855–3857.
[16] J. Vela, L.W. Zhu, C.J. Flaschenriem, W.W. Brennessel, R.J. Lachicotte, P.L. Holland, Organometallics 26 (2007) 3416–3423.
[17] L. Merle, M.F. Lappert, J.R. Severn, Chem. Rev. 102 (2002) 3031–3065.
[18] A.P. Dove, V.C. Gibson, E.L. Marshall, J.P. White, D.J. Williams, Dalton Trans. (2004) 570–578.
[19] J.E. Parks, R.H. Holm, Inorg. Chem. 7 (1968) 1408–1416.
[20] S.G. McGeachin, Can. J. Chem. 46 (1968) 1903–1911.
[21] C. William, J.C. Simon, K.C. Elaine, S.M. Francis, Angew. Chem. Int. Ed. 37 (1998) 796–798.
[22] Y. Yao, M. Xue, Y. Luo, Z. Zhang, R. Jiao, Y. Zhang, Q. Shen, W. Wong, K. Yu, J. Sun, J. Organomet. Chem. 678 (2003) 108–116.
[23] K.H. Park, W.J. Marshall, J. Org. Chem. 70 (2005) 2075–2081.
[24] H. Hamaki, N. Takeda, T.Y. amasaki, T. Sasamori, N. Tokitoh, J. Organomet. Chem. 692 (2007) 44–54.
[25] S. Fustero, M.G. Torre, B. Pina, A.S. Fuentes, J. Org. Chem. 64 (1999) 5551–5556.
[26] B. Deelman, P.B. Hitchcock, M.F. Lappert, W. Leung, H. Lee, T. Mak, J. Organomet. Chem. 513 (1996) 281–285.
[27] B. Deelman, P.B. Hitchcock, M.F. Lappert, W. Leung, H. Lee, T. Mak, Organometallics 18 (1999) 1444–1452.
[28] M. Rahim, N.J. Taylor, S. Xin, S. Collins, Organometallics 17 (1998) 1315–1323.
[29] R. Andrés, E.F. Jesús, J. Mata, J.C. Flores, R. Gómez, J. Organomet. Chem. 690 (2005) 939–940.
[30] R. Vollmerhaus, M. Rahim, R. Tomaszewski, S. Xin, N.J. Taylor, S. Collins, Organometallics 19 (2000) 2161–2169.
[31] L. Kakaliou, W.J. Scanlon, B. Qian, S.W. Baek, M.R. Smith, Inorg. Chem. 38 (1999) 5964–5977.
[32] F. Basuli, U.J. Kilgore, D. Brown, J.C. Huffman, D.J. Mindiola, Organometallics 23 (2004) 6166–6175.
[33] B. Qian, W.J. Scanlon, M.R. Smith, Oganometallics 18 (1999) 1693–1698.
[34] P.L. Franceschini, M. Morstein, H. Berke, H.W. Schmalle, Inorg. Chem. 42 (2003) 7273–7282.
[35] X. Jin, B.M. Novak, Macromolecules 33 (2000) 6205–6207.
[36] M. Zhou, S. Huang, L. Weng, W. Sun, D. Liu, J. Organomet. Chem. 665 (2003) 237–245.
[37] G. Xie, C. Qian, J. Polym. Sci. A: Polym. Chem. 46 (2008) 211–217.
[38] P.H. Budzelaar, B.V. Oorta, A.G. Orpenb, Eur. J. Inorg. Chem. (1998) 1485–1494.
[39] W.K. Kim, M.J. Fevola, L.M. Liable-Sands, A.L. Rheingold, K.H. Theopold, Organometallics 17 (1998) 4541–4543.
[40] G.B. Nikiforov, H.W. Roesky, J. Magull, T. Labahn, D. Vidovic, M. Noltemeyer, H. Schmidt, N.S. Hosmane, Polyhedron 22 (2003) 2669–2681.
[41] B.C. Bailey, F. Basuli, J.C. Huffman, D.J. Mindiola, Organometallics 25 (2006) 3963–3968.
[42] Y. Li, H. Gao, Q. Wu, J. Polym. Sci. A: Polym. Chem. 46 (2008) 93–101.
[43] L. Tang, Y. Duan, X. Li, Y. Li, J. Organomet. Chem. 691 (2006) 2023–2031.
[44] Y. Tohi, H. Makio, S. Matsui, M. Onda, T. Fujita, Macromolecules 36 (2003) 523–525.
[45] S. Gong, H. Ma, Dalton Trans. (2008) 3345–3357.
[46] M. Stender, R.J. Wright, B.E. Eichler, J. Prust, M.M. Olmstead, H.W. Roesky, P.P. Power, J. Chem. Soc., Dalton Trans. (2001) 3465–3469.
[47] X. Yang, Y. Zhang, J. Huang, J. Mol, Catal. A: Chem. 250 (2006) 145–152.
[48] The zirconium complex bearing *meta*-trifluoromethyl substituted **1j** could not be isolated as analytically pure sample according to the similar synthetic procedure as **2c**, so the mixture of complex (BDI-**1j**)$_2$ZrCl$_2$ and produced LiCl was used directly to carry out the ethylene polymerization experiment.
[49] N. Suzuki, Y. Masubuchi, Y. Yamaguchi, T. Kase, T. Miyamoto, A. Horiuchi, T. Mise, Macromolecules 33 (2000) 754–759.
[50] S. Ishii, J. Saito, S. Matsuura, Y. Suzuki, R. Furuyama, M. Mitani, T. Nakano, N. Kashiwa, T. Fujita, Macromol. Rapid Commun. 23 (2002) 693–697.
[51] Y. Yoshida, S. Matsui, Y. Takagi, M. Mitani, T. Nakano, H. Tanaka, N. Kashiwa, T. Fujita, Organometallics 20 (2001) 4793–4799.
[52] J. Saito, M. Onda, S. Matsui, M. Mitani, R. Furuyama, H. Tanaka, T. Fujita, Macromol. Rapid Commun. 23 (2002) 1118–1123.
[53] J. Saito, Y. Suzuki, H. Makio, H. Tanaka, M. Onda, T. Fujita, Macromolecules 39 (2006) 4023–4031.
[54] B. Rieger, C. Troll, J. Prouschen, Macromolecules 35 (2002) 5742–5743.
[55] M. Weiser, M. Wesolek, R. Mulhaupt, J. Organomet. Chem. 691 (2006) 2945–2952.
[56] L.E. Manzer, Inorg. Synth. 21 (1982) 135–136.
[57] P. Francis, R. Cooke, J. Elliott, J. Polym. Sci. 31 (1958) 453–466.
[58] *SADABS*, Bruker Nonius area detector scaling and absorption correction-V2.05, Bruker AXS Inc., Madison, WI, 1996.
[59] G.M. Sheldrick, SHELXTL 5.10 for windows NT, Structure Determination Software Programs, Bruker Analytical X-ray Systems, Inc, Madison, WI, 1997.
[60] *SAINT*, Version 6.02; Bruker AXS Inc.: Madison, WI, 1999.
[61] G.M. Sheldrick, SHELXS-97, Program for the Solution of Crystal Structures, University of Gottingen, Germany, 1990.
[62] G.M. Sheldrick, SHELXL-97, Program for the Refinement of Crystal Structures, University of Gottingen, Germany, 1997.